

Geophysical Research Letters

RESEARCH LETTER

10.1002/2014GL059962

Key Points:

- Heterogeneous nitryl chloride chemistry is implemented into a hemispheric model
- The largest enhancements of nitryl chloride occur over China and Western Europe
- Nitryl chloride subsequently affects tropospheric chemistry

Correspondence to:

G. Sarwar,
sarwar.golam@epa.gov

Citation:

Sarwar, G., H. Simon, J. Xing, and R. Mathur (2014), Importance of tropospheric ClNO_2 chemistry across the Northern Hemisphere, *Geophys. Res. Lett.*, 41, 4050–4058, doi:10.1002/2014GL059962.

Received 20 MAR 2014

Accepted 2 MAY 2014

Accepted article online 6 MAY 2014

Published online 2 JUN 2014

Importance of tropospheric ClNO_2 chemistry across the Northern Hemisphere

Golam Sarwar¹, Heather Simon², Jia Xing¹, and Rohit Mathur¹

¹National Exposure Research Laboratory, U.S. Environmental Protection Agency, RTP, North Carolina, USA, ²Office of Air Quality Planning and Standard, U.S. Environmental Protection Agency, RTP, North Carolina, USA

Abstract Laboratory and field experiments have revealed that uptake of dinitrogen pentoxide (N_2O_5) on aerosols containing chloride produces nitryl chloride (ClNO_2) and nitric acid. We incorporate heterogeneous ClNO_2 formation into the hemispheric Community Multiscale Air Quality model. This heterogeneous chemistry substantially enhances ClNO_2 levels in several areas of the Northern Hemisphere and alters the composition of airborne reactive nitrogen, comprising more than 15% of monthly mean values in some areas. Model results suggest that this heterogeneous chemistry reduces monthly mean total nitrate by up to 25% and enhances monthly mean daily maximum 8 h ozone by up to 7.0 ppbv. The pathway also enhances hydroxyl radical by more than 20% in some locations which in turn increases sulfate and other secondary pollutants. The largest ClNO_2 concentrations and impacts occur over China and Western Europe, two areas in which few relevant field measurements have been made.

1. Introduction

Nitryl chloride (ClNO_2) builds up in the boundary layer at night and subsequently undergoes photolysis in the morning to produce chlorine radicals (Cl^{\cdot}) and nitrogen dioxide (NO_2). Consequently, ClNO_2 has been shown to be both an important radical source [Osthoff *et al.*, 2008; Thornton *et al.*, 2010; Phillips *et al.*, 2012; Riedel *et al.*, 2012; Young *et al.*, 2012] and an important component of total reactive nitrogen (NO_x) [Osthoff *et al.*, 2008; Thornton *et al.*, 2010; Mielke *et al.*, 2011, 2013; Sarwar *et al.*, 2012]. One study found that under certain ambient early morning conditions, more chlorine radicals are formed from ClNO_2 photolysis than the hydroxyl radicals (HO) formed from ozone (O_3) photolysis [Phillips *et al.*, 2012]. Another study suggests that ClNO_2 photolysis may produce more radicals than nighttime nitrous acid formation and its subsequent photolysis in the morning [Young *et al.*, 2012]. Chlorine radicals react with organic compounds leading to O_3 production. NO_2 cycled through ClNO_2 also leads to O_3 production. Thus, elevated atmospheric ClNO_2 enhances O_3 production in the atmosphere as shown by Simon *et al.* [2009] and Sarwar *et al.* [2012].

Laboratory studies suggest that ClNO_2 forms from the uptake of dinitrogen pentoxide (N_2O_5) on aerosols containing chloride [Bertram and Thornton, 2009; Roberts *et al.*, 2009]. Traditionally, the uptake of N_2O_5 on aerosols was believed to primarily produce nitric acid (HNO_3). Consequently, the ClNO_2 chemical pathway can affect total nitrate ($\text{TNO}_3 = \text{HNO}_3 + \text{particulate nitrate}$) as shown by Sarwar *et al.* [2012].

Osthoff *et al.* [2008] first measured atmospheric ClNO_2 in 2006 and reported a peak value of about 1.2 ppbv near Houston, Texas. Riedel *et al.* [2012] also reported elevated levels of ClNO_2 in Los Angeles, California. Other investigators have found substantial ambient concentrations of ClNO_2 in areas distant from marine influence [Thornton *et al.*, 2010; Mielke *et al.*, 2011; Phillips *et al.*, 2012; Riedel *et al.*, 2013].

While there are a growing number of studies which have measured ambient ClNO_2 concentrations and studied both its formation and its impact on tropospheric chemistry, most have been conducted in locations throughout North America including Houston [Osthoff *et al.*, 2008], Los Angeles [Riedel *et al.*, 2012; Mielke *et al.*, 2013], Colorado [Thornton *et al.*, 2010; Riedel *et al.*, 2013], Long Island Sound [Kercher *et al.*, 2009], and Calgary [Mielke *et al.*, 2011]. A limited number of photochemical modeling studies have also focused on North America [Simon *et al.*, 2009, 2010; Sarwar *et al.*, 2012]. Only two measurement studies and no modeling studies have examined effects of tropospheric ClNO_2 chemistry outside of North America: one study in the North Atlantic [Kercher *et al.*, 2009] and one in Frankfurt, Germany [Phillips *et al.*, 2012]. Photochemical models provide a means to examine chemistry over much larger

spatial extents than is feasible with specialized measurement studies and can identify times and locations where ClNO_2 is most likely to play an important role in radical chemistry and nitrogen oxides (NO_x) cycling. In this work, for the first time, we assess the importance of the heterogeneous ClNO_2 production on tropospheric chemistry across the Northern Hemisphere (NH).

2. Method

2.1. Model Description and Application

The study uses the Community Multiscale Air Quality (CMAQ) model (version 5.0.2) to assess the impacts of ClNO_2 on air quality. The details of CMAQ have been described elsewhere [Foley *et al.*, 2010; Byun and Schere, 2006; Binkowski and Roselle, 2003]. Many studies have demonstrated the skill of the CMAQ model in simulating air quality [Eder and Yu, 2006; Appel *et al.*, 2007, 2008, 2012; Sarwar *et al.*, 2008, 2013, 2014; Foley *et al.*, 2010]. The horizontal extent of the modeling domain covered the entire NH and was discretized using a grid of 108 km resolution using a polar stereographic coordinate system, while the vertical extent of the model extended from surface to 5 kPa and contained 44 layers [Mathur *et al.*, 2011, 2014]. Meteorological fields for the study were prepared using the Weather Research and Forecasting (version 3.3) model [Skamarock *et al.*, 2008]. Model simulations were conducted for 2 months in winter (December 2005 to January 2006) and 2 months in summer (May–June 2006). The first month in each season was used as spin-up period; results for the subsequent months in winter and summer are presented. Each simulation used the 2005 version of the Carbon Bond (CB05) chemical mechanism with updated toluene chemistry [Whitten *et al.*, 2010]. The reaction mechanism also included gas-phase chlorine chemistry as well as the uptake of N_2O_5 on aerosols [Sarwar *et al.*, 2012]. The chlorine chemistry includes 25 gas-phase chemical reactions of Cl^- with organic and inorganic species including the formation of the ClONO isomer from the reaction of NO_2 and Cl^- [Leu, 1984] as well as the photolysis of ClNO_2 . We expect ClONO and ClNO_2 to behave similarly, so we use ClNO_2 to represent both in the model. Two different simulations were performed for each time period as follows. In the first simulation, the uptake of N_2O_5 on aerosols only produced HNO_3 . In the second simulation, the heterogeneous formation of ClNO_2 was turned on; thus, the uptake of N_2O_5 on aerosols containing chloride produced both HNO_3 and ClNO_2 . The difference in the model results were attributed to the heterogeneous ClNO_2 formation chemistry.

The study uses anthropogenic emissions from the Emissions Database for Global Atmospheric Research (<http://edgar.jrc.ec.europa.eu/index.php>) and biogenic emissions from Global Emissions Initiative (<http://www.geiacenter.org>). The model includes two major sources of particulate chloride: sea salts and biomass burning. The CMAQ model uses the parameterization of Gong [2003] for calculating sea-salt emissions [Kelly *et al.*, 2010]. Emissions of particulate chloride from biomass burning activity were based on Lobert *et al.* [1999]. These biomass burning emissions include the following source categories: savanna fires, wood and charcoal burning, deforestation, agro-industrial and dung burning, forest wildfires, slash and burn/shifting cultivation, burning in the fields, shrubland, heath, tundra fires, and grassland fires [Lobert *et al.*, 1999]. These estimates likely represent the upper limit of the biomass burning emissions. However, many other sources including those of power generation emit particulate chloride [Reff *et al.*, 2009]. Global emissions estimates of these other sources are not currently available and consequently are not included in this study. Thus, the results presented herein do not reflect the full impact of the ClNO_2 chemistry since particulate chloride emissions from industrial sources are not included. The CMAQ model uses three modes to describe the aerosol size distribution: Aitken mode, accumulation mode, and coarse mode. Sea-salt emissions are apportioned into accumulation mode and coarse mode particles, while biomass burning emissions are apportioned only into accumulation mode particles. Calculated sea-salt-derived accumulation mode particulate chloride emissions for the NH are 1.6 Tg in January and 0.77 Tg in June, while sea-salt-derived coarse mode particulate chloride emissions are 102 Tg in January and 46.6 Tg in June. Accumulation mode particulate chloride emissions from biomass burning are 0.4 Tg in January and 0.4 Tg in June. Sea salt contributes substantially more to the total particulate chloride emissions than biomass burning activity in coastal and marine environments.

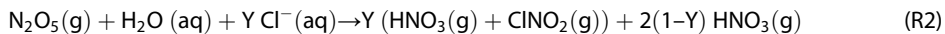
2.2. Heterogeneous ClNO_2 Formation Chemistry

The standard CMAQv5.0.2 model includes the uptake of N_2O_5 on aerosols to produce HNO_3 as the only reaction product (R1). It uses the Davis *et al.* [2008] parameterization for the heterogeneous uptake

coefficient of N_2O_5 ($\gamma_{\text{N}_2\text{O}_5}$) and accounts for the heterogeneous conversion of N_2O_5 on Aitken mode and accumulation mode aerosols.



Finlayson-Pitts et al. [1989], Bertram and Thornton [2009], and Roberts et al. [2009] suggest that when particles contain chloride, the uptake of N_2O_5 also produces ClNO_2 as a reaction product (R2).



The yield of ClNO_2 (Y) depends on particulate chloride concentration $[\text{Cl}^-]$ and particle liquid water content $[\text{H}_2\text{O}(\text{l})]$ and has been parameterized by *Bertram and Thornton [2009]* and *Roberts et al. [2009]* (equation (1)). *Bertram and Thornton [2009]* measured a constant of 483, while *Roberts et al. [2009]* measured a constant of 485 for use in equation (1):

$$Y = \frac{1}{1 + \frac{1}{483[\text{Cl}^-]}} \quad (1)$$

Bertram and Thornton [2009] also suggested that the presence of particulate chloride alters $\gamma_{\text{N}_2\text{O}_5}$ and developed the following parameterization (equation (2)):

$$\gamma_{\text{N}_2\text{O}_5} = 3.2 \times 10^{-8} k \left(1 - \frac{1}{\left(\frac{0.06[\text{H}_2\text{O}(\text{l})]}{[\text{NO}_3^-]} \right) + 1 + \left(\frac{29[\text{Cl}^-]}{[\text{NO}_3^-]} \right)} \right) \quad (2)$$

where $[\text{H}_2\text{O}(\text{l})]$ = particle liquid water (mol/L), $[\text{NO}_3^-]$ = particulate nitrate (mol/L), $[\text{Cl}^-]$ = particulate chloride (mol/L), and k represents the rate coefficient for the disassociation of N_2O_5 (aq) and is calculated as follows:

$$k = 1.15 \times 10^6 - 1.15 \times 10^6 e^{-0.13x[\text{H}_2\text{O}(\text{l})]} \quad (3)$$

Bertram et al. [2009] compared the $\gamma_{\text{N}_2\text{O}_5}$ parameterization from equation (2) to measurements made on ambient aerosols and found that when organic content was low, relative humidity was a primary controller of $\gamma_{\text{N}_2\text{O}_5}$ while nitrate concentration was a secondary controller. Since the *Bertram and Thornton [2009]* parameterization does not explicitly account for the effects of organics, the heterogeneous uptake coefficient may be overestimated when organic aerosol concentrations are high. The effect of not accounting for organic inhibition of N_2O_5 uptake should be most pronounced in summer and less pronounced in winter. In this study, we replace (R1) with (R2) in the CMAQ model and replace the *Davis et al. [2008]* parameterization with the *Bertram and Thornton [2009]* formulation for $\gamma_{\text{N}_2\text{O}_5}$. The yields and heterogeneous uptake coefficients are calculated separately on Aitken, accumulation, and coarse particles using equations (1) and (2), respectively.

3. Results and Discussion

3.1. Predicted ClNO_2 Levels and the Composition of Total Reactive Nitrogen

ClNO_2 forms at night and tends to peak before the sunrise. Predicted levels decrease rapidly after sunrise and reach a minimum value during the day. Monthly mean of nightly 1 h maximum ClNO_2 levels without and with the heterogeneous production are shown in Figure 1. Predicted ClNO_2 levels formed via the gas-phase reaction of $\text{NO}_2 + \text{Cl}$ are small (<1 parts per trillion by volume (pptv)) as shown in Figures 1a and 1b. The inclusion of the heterogeneous formation reaction enhances predicted ClNO_2 levels in many areas by more than 3 orders of magnitude. Collocation of anthropogenic NO_x sources and particulate chloride from sea salt triggers the heterogeneous production of ClNO_2 in coastal areas, while NO_x and particulate chloride from biomass burning activity activates the heterogeneous production of ClNO_2 over inland areas.

Predicted surface-level winter ClNO_2 values are greater than those in summer due to higher N_2O_5 levels, higher ClNO_2 yields, and lower mixing height. The colder winter temperature shifts the $\text{N}_2\text{O}_5-\text{NO}_3$ equilibrium toward N_2O_5 , and the longer winter nights lead to more N_2O_5 accumulation in dark conditions. The monthly mean ClNO_2 yields range between 0.5 and 1.0 across most of the NH in winter, with values greater than 0.75

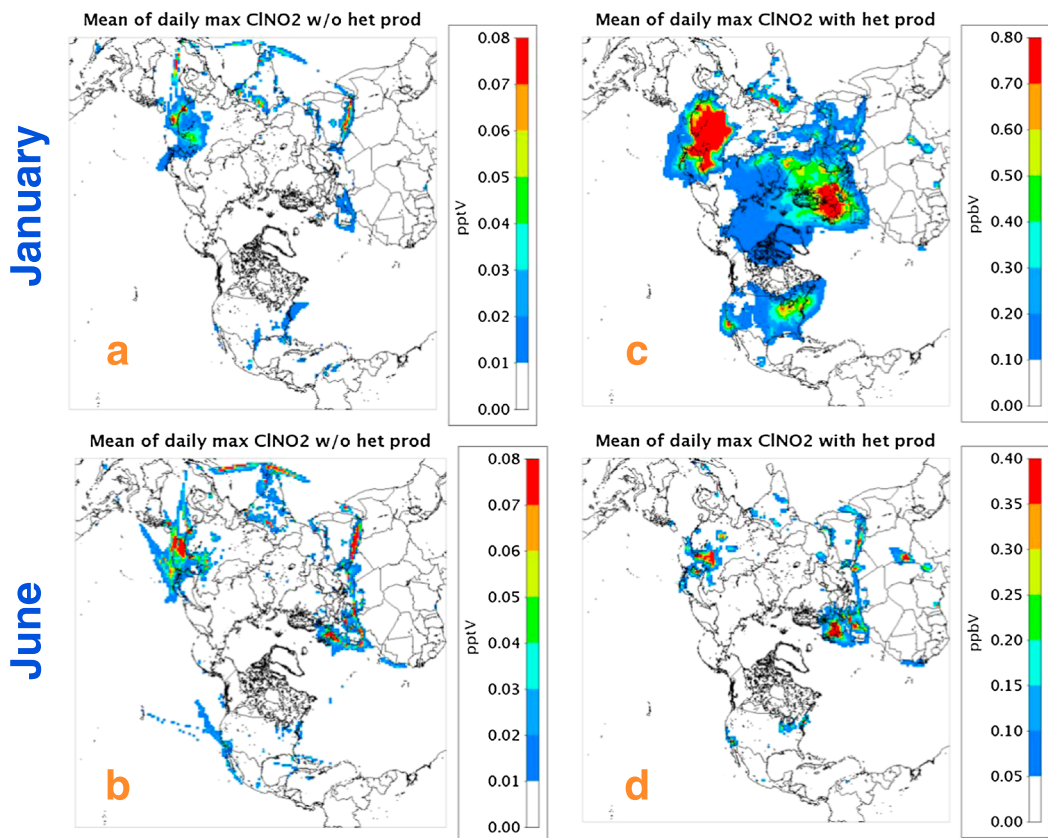


Figure 1. (a) Mean of nightly 1 h maximum CINO₂ in January without the heterogeneous CINO₂ production (pptv), (b) mean of nightly 1 h maximum CINO₂ in June without the heterogeneous CINO₂ production (pptv), (c) mean of nightly 1 h maximum CINO₂ in January with the heterogeneous CINO₂ production (ppbv), and (d) mean of nightly 1 h maximum CINO₂ in June with the heterogeneous CINO₂ production (ppbv). Note that scales for Figures 1a and 1b are given in units of parts per trillion by volume, while scales in Figures 1c and 1d are given in units of parts per billion by volume.

over the Oceans, China, parts of Africa, and the southwestern United States. These high winter CINO₂ yields and N₂O₅ concentrations lead to monthly mean nightly maximum winter CINO₂ levels of more than 0.7 ppbv over large areas of China and Western Europe. The heterogeneous CINO₂ formation pathway also produces more than 0.4 ppbv of winter CINO₂ over parts of India, Western Europe, the eastern United States, and Southern California. In contrast, N₂O₅, CINO₂ yields, and resulting CINO₂ concentrations are lower in the summer. Monthly mean CINO₂ yields range between 0 and 1.0 in the summer with values of 0.1–0.6 over Europe and the United States and 0.5–1.0 over China. This results in summer CINO₂ concentrations of up to 0.4 ppbv only over small areas of China and Western Europe. Predicted summer levels elsewhere in the NH are small compared to those obtained in winter. However, values greater than 200 pptv are predicted in some areas.

Predicted peak CINO₂ levels from the current study are compared to the measured peak values from field studies in Table 1. While predicted winter levels tend to be closer to the observed data, summer levels are lower than the observations. Similar model calculations using the same chemistry but at a finer grid resolution (12 km) over the United States [Sarwar *et al.*, 2012] predicted higher CINO₂ concentrations (especially in the summer) which matched reasonably well with measurements in the United States suggesting that local peaks are likely smoothed out by the coarser grid resolution (108 km) used in this study. In addition, the coarse grid resolution may dampen localized O₃ titration due to artificial dilution of urban NO_x emissions and thus could cause an underestimate of nighttime NO₃ and consequently N₂O₅ formation. Therefore, the modeling results presented here may not capture the largest CINO₂ effects.

The heterogeneous production of CINO₂ sequesters NO_x which would otherwise form HNO₃ and be lost quickly from the atmosphere via deposition. Upon sunrise, CINO₂ undergoes photolysis liberating NO_x and

Table 1. A Comparison of Predicted ClNO_2 Concentrations to Observed Data^a

Location	Date	Peak Observation (pptv)	Peak Predictions (pptv)		References
			January, 2006	June, 2006	
Houston, TX, USA	Aug–Sep 2008	1200	1100	150	Osthoff <i>et al.</i> [2008]
Boulder, CO, USA	Feb 2009	450	400	70	Thornton <i>et al.</i> [2010]
Boulder, CO, USA	Feb–Mar 2011	1300	400	70	Riedel <i>et al.</i> [2013]
Los Angeles, CA, USA (marine)	May–Jun 2010	2100	2300	600	Riedel <i>et al.</i> [2012]
Pasadena, CA, USA (inland)	May–Jun 2010	3600	1600	700	Mielke <i>et al.</i> [2013]
Long Island Sound	Mar 2008	200	1300	1400	Kercher <i>et al.</i> [2009]
North Atlantic	Mar 2008	100	2100	600	Kercher <i>et al.</i> [2009]
Calgary, Alberta, Canada	Apr 2010	250	300	30	Mielke <i>et al.</i> [2011]
Frankfurt, Germany	Aug–Sep 2011	800	1300	800	Phillips <i>et al.</i> [2012]

^aNote that observed and model values are not paired in time and space. Model predictions are taken from the general geographic areas of observed data.

Cl ; both of which affect atmospheric chemistry. The production of ClNO_2 alters the relative composition of NO_y . TNNO_3 is the largest contributor to the NO_y budget in the model's surface layer and accounts for 54% and 51% of the total NO_y in winter and summer, respectively. NO_x is the second largest contributor to the NO_y budget and accounts for 23% of the total NO_y in winter as well as in summer. In winter, nitrous acid accounts for 0.2%, peroxyacetyl nitrate for 8.7%, higher peroxyacetyl nitrate for 5.8%, and peroxynitric acid for 0.5% of NO_y averaged over the entire NH. In contrast, ClNO_2 accounts for 2.9% of NO_y ; thus, its contribution to NO_y is more than that of nitrous acid or peroxynitric acid and is half of the higher peroxyacetyl nitrate. In summer, nitrous acid accounts for 0.2%, peroxyacetyl nitrate for 12.3%, higher peroxyacetyl nitrate for 7.8%,

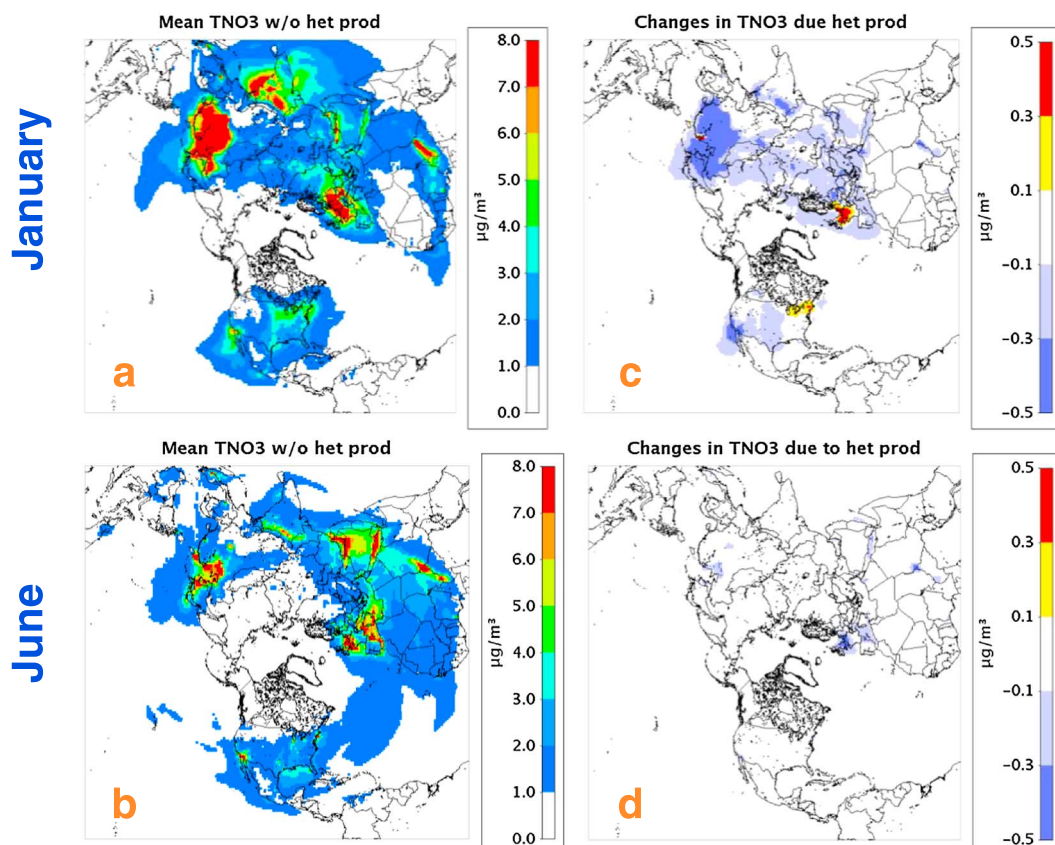


Figure 2. (a) Mean TNNO_3 in January without the heterogeneous ClNO_2 production, (b) mean TNNO_3 in June without the heterogeneous ClNO_2 production, (c) changes in mean TNNO_3 in January due to the heterogeneous ClNO_2 production, and (d) changes in mean TNNO_3 in June due to the heterogeneous ClNO_2 production.

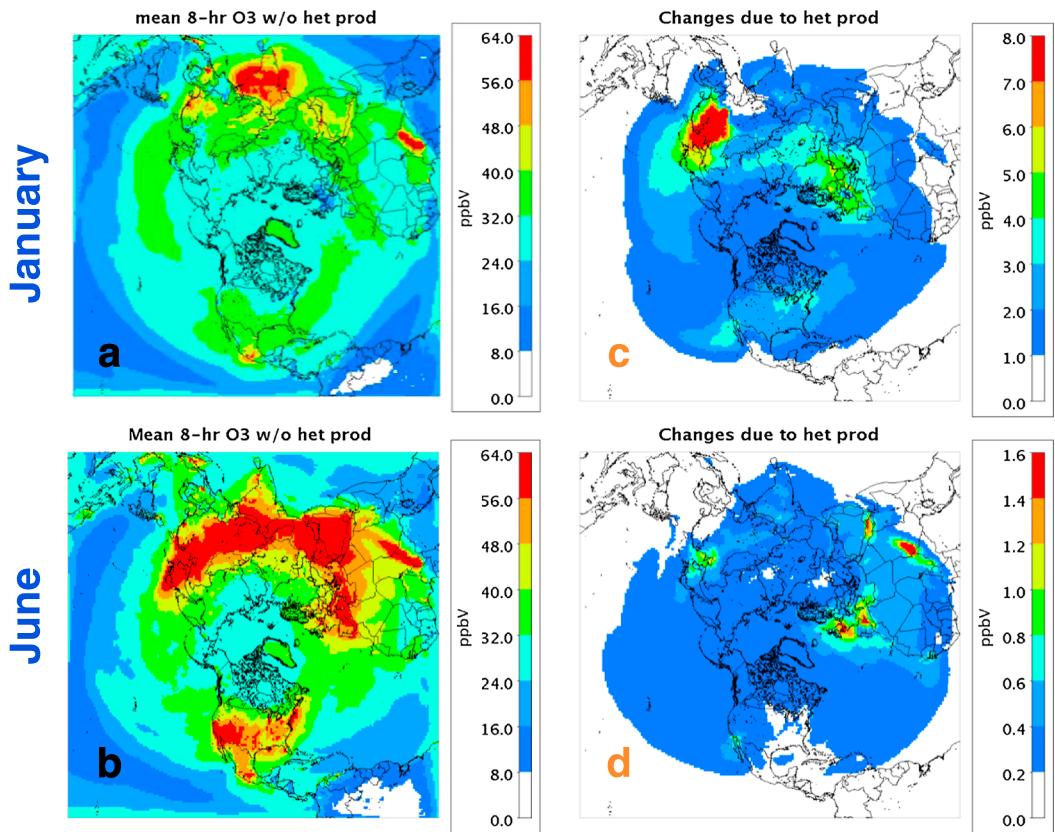


Figure 3. (a) Mean of daily maximum 8 h O₃ in January without the heterogeneous C₁N₀₂ production, (b) mean of daily maximum 8 h O₃ in June without the heterogeneous C₁N₀₂ production, (c) changes in mean daily maximum 8 h O₃ in January due to the heterogeneous C₁N₀₂ production, and (d) changes in mean daily maximum 8 h O₃ in June due to the heterogeneous C₁N₀₂ production.

peroxynitric acid for 0.1%, and C₁N₀₂ for 0.1% of NO_y averaged over the entire NH. Hence, summer C₁N₀₂ levels are similar to those of peroxy nitric acid. Thus, C₁N₀₂ accounts for a moderate fraction of the NO_y budget even when averaged over the entire NH. It, however, can comprise a larger fraction of NO_y in localized areas. For example, C₁N₀₂ accounts for more than 6% of winter NO_y over large areas of China and more than 15% of winter NO_y in Scandinavia and northern Russia. These seasonal and regional differences in the NO_y composition then impact NO_x recycling in the troposphere affecting both oxidant and particle formation as discussed next.

3.2. Impact of the C₁N₀₂ Production on Total Nitrate

Figure 2 displays the monthly mean TNO₃ levels without the heterogeneous production of C₁N₀₂ and changes due to the heterogeneous C₁N₀₂ formation chemistry. Winter TNO₃ levels without the heterogeneous C₁N₀₂ formation chemistry exceed 7.0 $\mu\text{g m}^{-3}$ over a large area in China, India, Western Europe, and Africa. More than 3.0 $\mu\text{g m}^{-3}$ of TNO₃ is predicted over areas of eastern and western United States. In most areas, summer TNO₃ levels are lower than the corresponding winter values. The heterogeneous C₁N₀₂ production decreases winter TNO₃ by 0.3–0.5 $\mu\text{g m}^{-3}$ over much of China, India, Western Europe, and western U.S. Although not visible in the figure, the heterogeneous C₁N₀₂ production decreases winter TNO₃ by as much as 2.0–3.0 $\mu\text{g m}^{-3}$ at some locations in China. C₁N₀₂ formation can also increase winter TNO₃ due to recycled NO_x from C₁N₀₂ photolysis as well as enhanced HO levels which, in turn, enhance daytime production of HNO₃ via the homogeneous reaction of NO₂ + HO. In most locations, the reductions in nighttime heterogeneous production of HNO₃ outweigh the increases in the daytime homogeneous HNO₃ production, and thus, C₁N₀₂ chemistry reduces winter TNO₃ levels. However, in some isolated locations, C₁N₀₂ increases winter TNO₃ levels. The impact of C₁N₀₂ chemistry on summer

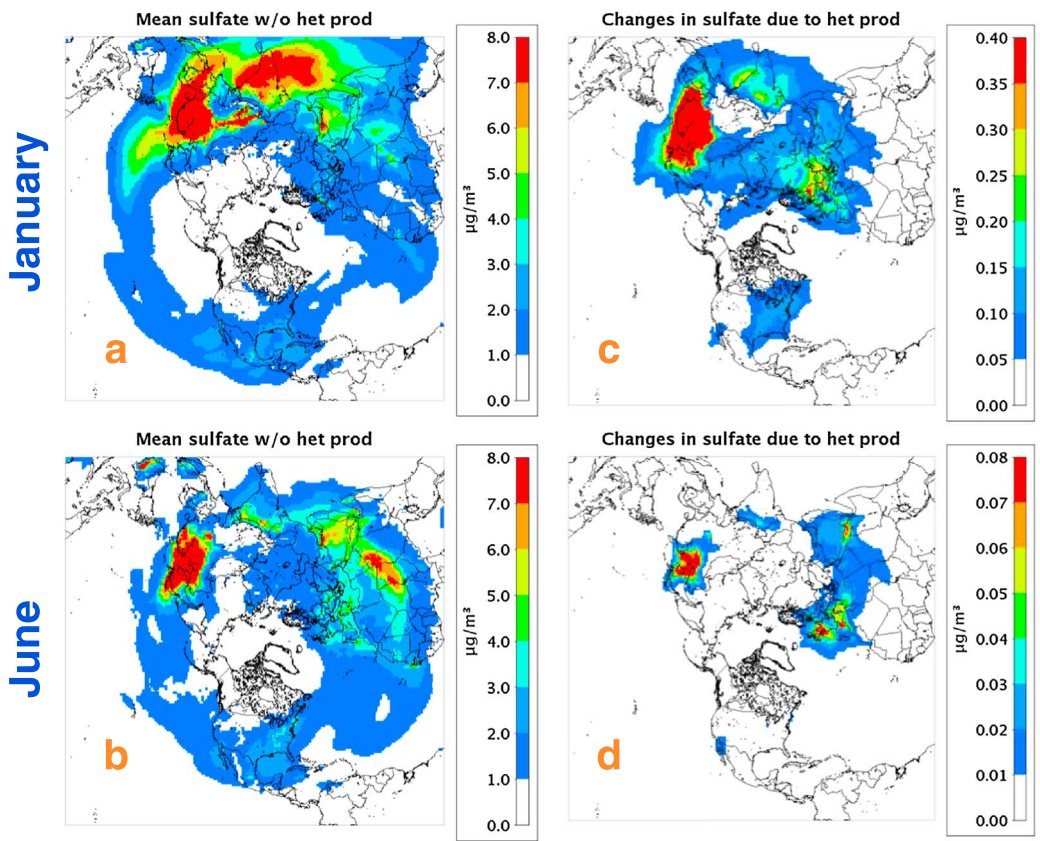


Figure 4. (a) Mean sulfate in January without the heterogeneous CINO_2 production, (b) mean sulfate in June without the heterogeneous CINO_2 production, (c) changes in mean sulfate in January due to the heterogeneous CINO_2 production, and (d) changes in mean sulfate in June due to the heterogeneous CINO_2 production.

TNO_3 is limited to much more localized areas in Europe, Africa, and China. CINO_2 production decreases winter TNO_3 by 3.3% and summer TNO_3 by 0.3% averaged over the entire NH but by up to 25% and 7% in some locations.

3.3. Impact of the CINO_2 Production on Ozone

The monthly mean of daily maximum 8 h O_3 levels without the heterogeneous production of CINO_2 and changes due to the CINO_2 chemistry are shown in Figure 3. Ozone concentrations are highest in the summer near high population areas and are lower during winter over remote areas. Heterogeneous CINO_2 formation chemistry enhances both the winter and summer O_3 ; however, the enhancements are greater in winter (>7.0 ppbv increase in monthly mean of 8 h daily maximum over a large area in China and 1.0–6.0 ppbv in the rest of the NH). CINO_2 formation enhances summer O_3 by only 0.2–1.6 ppbv.

3.4. Impact on Hydroxyl Radical and Subsequent Impact on Other Chemical Species

Heterogeneous CINO_2 formation chemistry enhances both winter and summer HO levels. This chemistry increases winter HO by 3.5% and summer HO by 0.3% averaged over the entire NH. The increased HO can occur through several chemical pathways. First, as described in section 3.3, CINO_2 enhances O_3 which in turn produces more singlet oxygen atom (O^1D) via photolysis. Additional O^1D leads to enhanced HO via its reaction with water vapor. Second, photolysis of CINO_2 produces Cl^- which subsequently oxidizes volatile organic compounds and, in turn, also leads to more HO. While on average, winter HO is enhanced by 3.5%, larger increases occur in isolated areas. For example, winter HO over localized areas of China, Europe, United States, and Canada increases by more than 20% compared to the simulation without heterogeneous CINO_2 formation chemistry. These findings are consistent with box model results constrained by measurements made in Los Angeles, CA, which show CINO_2 increasing morning HO levels by 25% [Riedel *et al.*, 2013].

Enhanced HO leads to increased secondary pollutants such as sulfate through the oxidation of sulfur dioxide. The monthly mean sulfate without the heterogeneous production of ClNO_2 and changes due to the ClNO_2 chemistry are shown in Figure 4. The inclusion of heterogeneous ClNO_2 formation chemistry enhances winter monthly sulfate by $>0.35 \mu\text{g m}^{-3}$ over China, $>0.20 \mu\text{g m}^{-3}$ over India and Western Europe, and $>0.05 \mu\text{g m}^{-3}$ over United States. This chemistry also enhances summer sulfate though its impact is smaller and more localized than in winter.

4. Discussion

To our knowledge, this is the first study that examines the impact of the heterogeneous ClNO_2 production on air quality across the Northern Hemisphere. Predicted ClNO_2 can reach high levels (in the range of 1 ppb) in several areas across the NH, especially during winter, and can account for a sizeable fraction of the NO_y budget. Due to the large grid size used for hemispheric modeling, we may not fully capture peak ClNO_2 concentrations and its effects on tropospheric chemistry; thus, these modeling results may be considered a lower bound. Similar to previous modeling studies [Simon *et al.*, 2009; Sarwar *et al.*, 2012], this analysis shows that the resulting ClNO_2 alters air quality by decreasing total nitrate and enhancing O_3 . Sizable ClNO_2 concentrations also increase HO which subsequently enhances the atmospheric oxidation capacity and secondary air pollutant formation. This work expands on previous studies by characterizing ClNO_2 concentrations and effects across many portions of the NH which have not previously been evaluated. We identify winter in China and Western Europe as the season and locations in which ClNO_2 chemistry is likely to have the largest impact. Much of the ClNO_2 predicted to span large inland areas of China forms as a result of chloride present in biomass burning plumes. While this is an intriguing finding, no field or lab studies have measured ClNO_2 formation on this type of particle. Previous studies focused on locations where chloride from sea salt and other sources was present in aqueous particles, while at least some of the chlorine in biomass burning particles may be in other forms (e.g. covalently bonded in organic chlorine compounds). These results highlight the need for further measurement studies to verify whether ClNO_2 forms on the surface of biomass burning particles and to quantify its impacts at the times and locations where the model predicts it is most important. It also underscores the need for developing a more accurate global emissions inventory for particulate chloride.

Acknowledgments

The Community Multiscale Air Quality (CMAQ) model (CMAQv5.0.2) was used for generating the model results. The CMAQ model can be downloaded from <http://www.cmascenter.org>. Although this paper has been reviewed by EPA and approved for publication, it does not necessarily reflect EPA's policies or views.

The Editor thanks two anonymous reviewers for their assistance in evaluating this paper.

References

Appel, K. W., A. B. Gilliland, G. Sarwar, and R. C. Gilliam (2007), Evaluation of the Community Multiscale Air Quality (CMAQ) model version 4.5: Sensitivities impacting model performance, Part I—Ozone, *Atmos. Environ.*, 41, 9603–9615.

Appel, K. W., P. Bhave, A. Gilliland, G. Sarwar, and S. J. Roselle (2008), Evaluation of the Community Multiscale Air Quality model version 4.5: Uncertainties and sensitivities impacting model performance, Part II—Particulate Matter, *Atmos. Environ.*, 42, 6057–6066.

Appel, K. W., C. Chemel, S. J. Roselle, X. V. Francis, H. Rong-Ming, R. S. Sokhi, S. T. Rao, and S. Galmarini (2012), Examination of the Community Multiscale Air Quality (CMAQ) model performance over the North American and European domains, *Atmos. Environ.*, 53, 142–155.

Bertram, T. H., and J. A. Thornton (2009), Toward a general parameterization of N_2O_5 reactivity on aqueous particles: The competing effects of particle liquid water, nitrate and chloride, *Atmos. Chem. Phys.*, 9, 8351–8363, doi:10.5194/acp-9-8351-2009.

Bertram, T. H., J. A. Thornton, T. P. Riedel, A. M. Middlebrook, R. Bahreini, T. S. Bates, P. K. Quinn, and D. J. Coffman (2009), Direct observations of N_2O_5 reactivity on ambient aerosol particles, *Geophys. Res. Lett.*, 36, L19803, doi:10.1029/2009GL040248.

Binkowski, F. S., and S. J. Roselle (2003), Community Multiscale Air Quality (CMAQ) model aerosol component, I: Model description, *J. Geophys. Res.*, 108(D6), 4183, doi:10.1029/2001JD001409.

Byun, D., and K. L. Schere (2006), Review of the governing equations, computational algorithms, and other components of the Models-3 Community Multiscale Air Quality (CMAQ) modeling system, *Appl. Mech. Rev.*, 59, 51–77.

Davis, J. M., P. V. Bhave, and K. M. Foley (2008), Parameterization of N_2O_5 reaction probabilities on the surface of particles containing ammonium, sulfate, and nitrate, *Atmos. Chem. Phys.*, 8, 5295–5311, doi:10.5194/acp-8-5295-2008.

Eder, B., and S. Yu (2006), A performance evaluation of the 2004 release of Models-3 CMAQ, *Atmos. Environ.*, 40, 4811–4824.

Finlayson-Pitts, B. J., M. J. Ezell, and J. N. Pitts Jr. (1989), Formation of chemically active chlorine compounds by reactions of atmospheric NaCl particles with gaseous N_2O_5 and ClONO_2 , *Nature*, 337(6204), 241–244.

Foley, K. M., *et al.* (2010), Incremental testing of the Community Multiscale Air Quality (CMAQ) modeling system version 4.7, *Geosci. Model Dev.*, 3, 205–226, doi:10.5194/gmd-3-205-2010.

Gong, S. L. (2003), A parameterization of sea salt aerosol source function for sub- and super-micronparticles, *Global Biogeochem. Cycles*, 17(4), 1097, doi:10.1029/2003GB002079.

Kelly, J., P. Bhave, C. G. Nolte, U. Shankar, and K. Foley (2010), Simulating emission and chemical evolution of coarse sea salt particles in the Community Multiscale Air Quality (CMAQ) model, *Geosci. Model Dev.*, 3(1), 257–273.

Kercher, J. P., T. P. Riedel, and J. A. Thornton (2009), Chlorine activation by N_2O_5 : Simultaneous, in situ detection of ClNO_2 and N_2O_5 by chemical ionization mass spectrometry, *Atmos. Meas. Tech.*, 2, 193–204.

Leu, M. T. (1984), Kinetics of the reaction $\text{Cl} + \text{NO}_2 + \text{M}$, *Int. J. Chem. Kinet.*, 16(11), 1311–1319.

Loebert, J. M., W. C. Kenee, J. A. Logan, and R. Yevich (1999), Global chlorine emissions from biomass burning: Reactive chlorine emissions inventory, *J. Geophys. Res.*, 104(D7), 8373–8389, doi:10.1029/1998JD100077.

Mathur, R., R. C. Gilliam, R. Bullock, S. J. Roselle, J. E. Pleim, D. C. Wong, F. S. Binkowski, and D. G. Streets (2011), Extending the applicability of the Community Multiscale Air Quality model to hemispheric scales: Motivation, challenges, and progress, in *NATO/SPS/ITM Air Pollution Modeling and its Application XXI*, C Series, edited by D. G. Steyn and S. TriniGastelli, chap. 30, pp. 175–179, Springer, Houten, Netherlands.

Mathur, R., S. Roselle, J. Young, and D. Kang (2014), Representing the effects of long-range transport and lateral boundary conditions in regional air pollution models, in *Air Pollution Modeling and its Application XXII*, chap. 51, pp. 303–308, Springer, Heidelberg, Germany.

Mielke, L. H., A. Furgeson, and H. D. Osthoff (2011), Observation of ClNO_2 in a mid-continental urban environment, *Environ. Sci. Technol.*, 45, 8889–8896.

Mielke, L. H., et al. (2013), Heterogeneous formation of nitryl chloride and its role as a nocturnal NO_x reservoir species during CalNex-LA 2010, *J. Geophys. Res. Atmos.*, 118, 10,638–10,652, doi:10.1002/jgrd.50783.

Osthoff, H. D., et al. (2008), High levels of nitryl chloride in the polluted subtropical marine boundary layer, *Nat. Geosci.*, 1, 324–328.

Phillips, G. J., M. J. Tang, J. Thieser, B. Brickwedde, G. Schuster, B. Bohn, J. Lelieveld, and J. N. Crowley (2012), Significant concentrations of nitryl chloride observed in rural continental Europe associated with the influence of sea salt chloride and anthropogenic emissions, *Geophys. Res. Lett.*, 39, L10811, doi:10.1029/2012GL051912.

Reff, A., P. V. Bhave, H. Simon, T. G. Pace, G. A. Pouliot, J. D. Mobley, and M. Houyoux (2009), Emissions inventory of $\text{PM}_{2.5}$ trace elements across the United States, *Environ. Sci. Technol.*, 43, 5790–5796.

Riedel, T. P., et al. (2012), Nitryl chloride and molecular chlorine in the coastal marine boundary layer, *Environ. Sci. Technol.*, 46, 10,463–10,470.

Riedel, T. P., et al. (2013), Chlorine activation within urban or power plant plumes: Vertically resolved ClNO_2 and Cl_2 measurements from a tall tower in a polluted continental setting, *J. Geophys. Res. Atmos.*, 118, 8702–8715, doi:10.1002/jgrd.50637.

Roberts, J. M., H. D. Osthoff, S. S. Brown, A. R. Ravishankara, D. Coffman, P. Quinn, and T. Bates (2009), Laboratory studies of products of N_2O_5 uptake on Cl^- containing substrates, *Geophys. Res. Lett.*, 36, L20808, doi:10.1029/2009GL040448.

Sarwar, G., D. Luecken, G. Yarwood, G. Whitten, and B. Carter (2008), Impact of an updated Carbon Bond mechanism on air quality using the Community Multiscale Air Quality modeling system: Preliminary assessment, *J. Appl. Meteorol. Climatol.*, 47, 3–14.

Sarwar, G., H. Simon, P. Bhave, and G. Yarwood (2012), Examining the impact of heterogeneous nitryl chloride production on air quality across the United States, *Atmos. Chem. Phys.*, 12, 1–19.

Sarwar, G., J. Godowitch, B. H. Henderson, K. Fahey, G. Pouliot, W. T. Hutzell, R. Mathur, D. Kang, W. S. Goliff, and W. R. Stockwell (2013), A comparison of atmospheric composition using the Carbon Bond and Regional Atmospheric Chemistry Mechanisms, *Atmos. Chem. Phys.*, 13, 9695–9712.

Sarwar, G., H. Simon, K. Fahey, R. Mathur, W. S. Goliff, and W. R. Stockwell (2014), Impact of sulfur dioxide oxidation by Stabilized Criegee Intermediate on sulfate, *Atmos. Environ.*, 85, 204–214.

Simon, H., Y. Kimura, G. McGaughey, D. T. Allen, S. S. Brown, H. D. Osthoff, J. M. Roberts, D. Byun, and D. Lee (2009), Modeling the impact of ClNO_2 on ozone formation in the Houston area, *J. Geophys. Res.*, 114, D00F03, doi:10.1029/2008JD010732.

Simon, H., et al. (2010), Modeling heterogeneous ClNO_2 formation, chloride availability, and chlorine cycling in Southeast Texas, *Atmos. Environ.*, 44, 5476–5488.

Skamarock, W. C., J. B. Klemp, J. Dudhia, D. O. Grill, D. M. Barker, M. G. Duda, X.-Y. Huang, W. Wang, and J. G. Powers (2008), A description of the advanced research WRF version 3, *NCAR Tech Note NCAR/TN 475 STR*, UCAR Communications, Boulder, Colo.

Thornton, J. A., et al. (2010), A large atomic chlorine source inferred from mid-continental reactive nitrogen chemistry, *Nature*, 464, 271–274.

Whitten, G. Z., G. Heo, Y. Kimura, E. McDonald-Buller, D. T. Allen, W. P. L. Carter, and G. Yarwood (2010), A new condensed toluene mechanism for Carbon Bond: CB05-TU, *Atmos. Environ.*, 44, 5346–5355.

Young, C. J., et al. (2012), Vertically resolved measurements of nighttime radical reservoirs in Los Angeles and their contribution to the urban radical budget, *Environ. Sci. Technol.*, 46, 10,965–10,973.